Title
Trioxolane-Mediated Delivery of Mefloquine Limits Brain Exposure in a Mouse Model of Malaria

Journal
ACS Medicinal Chemistry Letters, 6(11)

ISSN
1948-5875

Authors
Lauterwasser, Erica MW
Fontaine, Shaun D
Li, Hao
et al.

Publication Date
2015-11-12

DOI
10.1021/acsmedchemlett.5b00296

Peer reviewed

ACS Medicinal Chemistry Letters

Letter

pubs.acs.org/acsmedchemlett

Trioxolane-Mediated Delivery of Mefloquine Limits Brain Exposure in a Mouse Model of Malaria

Erica M. W. Lauterwasser,[†,⊥] Shaun D. Fontaine,[†,#] Hao Li,[§] Jiri Gut,[‡] Kasiram Katneni,[∥] Susan A. Charman,[∥] Philip J. Rosenthal,[‡] Matthew Bogyo,[§] and Adam R. Renslo*[,†]

[†]Department of Pharmaceutical Chemistry and [‡]Department of Medicine, University of California San Francisco, 1700 Fourth Street, San Francisco, California 94158, United States

[§]Departments of Pathology and Microbiology and Immunology, Stanford School of Medicine, 300 Pasteur Drive, Stanford, California 94305, United States

[∥]Centre for Drug Candidate Optimisation, Monash Institute of Pharmaceutical Sciences, Monash University, Parkville, VIC 3052, Australia

Supporting Information

ABSTRACT: Peroxidic antimalarial agents including the sequiterpene artemisinins and the synthetic 1,2,4-trioxolanes function via initial intraparasitic reduction of an endoperoxide bond. By chemically coupling this reduction to release of a tethered drug species it is possible to confer two distinct pharmacological effects in a parasite-selective fashion, both in vitro and in vivo. Here we demonstrate the trioxolane-mediated delivery of the antimalarial agent mefloquine in a mouse malaria model. Selective partitioning of the trioxolane−mefloquine conjugate in parasitized erythrocytes, combined with effective exclusion of the conjugate from brain significantly reduced brain exposure as compared to mice directly administered mefloquine. These studies suggest the potential of trioxolane-mediated drug delivery to mitigate off-target effects of existing drugs, including the adverse neuropsychiatric effects of mefloquine use in therapeutic and chemoprophylactic settings.

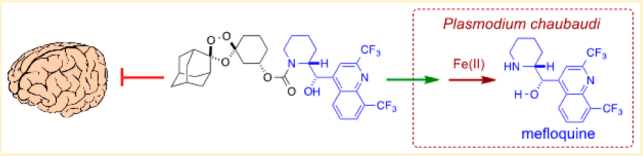

KEYWORDS: *antimalarial, trioxolane, mefloquine, drug delivery*

The antimalarial agent (±)-mefloquine (**1**) has for decades been a stalwart of antimalarial chemotherapy and chemoprophylaxis. While both enantiomers of **1** exhibit potent antiplasmodial effects,[1,2] one or both enantiomers have variously been reported to interact with CNS off-targets including gap junction channels, adenosine receptors, GABA receptors, and serotonin (5-HT) receptors, as recently reported by Riscoe and co-workers.[3] It seems clear that some aspect of this CNS pharmacology must account for the rare but serious neuropsychiatric side-effects of mefloquine use, which include anxiety, paranoia, depression, hallucinations, and psychotic behavior. Even so, **1** exhibits many favorable properties, particularly in the context of chemoprophylaxis, where its extended half-life enables convenient once-weekly dosing. The combination of a long-acting drug like **1** with a rapid-acting agent such as a 1,2,4-trioxolane (e.g., arterolane,[4] **2**) may be optimal for chemoprevention in malaria-endemic regions (Figure 1). Herein we describe **3**, a 3″-trioxolane conjugate of **1** that confers a trioxolane-based effect coincident with release of free **1**. We report that administration of **3** significantly reduces the exposure of **1** in the brains of treated mice, when compared to mice administered **1** directly. Our results thus suggest an approach to antimalarial chemoprophylaxis that combines rapid and prolonged antimalarial activities with superior tolerability.

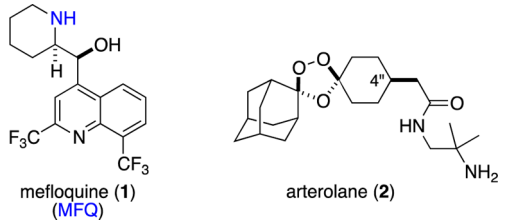

Figure 1. Mefloquine and arterolane. The (+)-(11*S*,12*R*) enantiomer of mefloquine is shown.

In recent years, our group and others have sought to exploit the intrinsic reactivity of endoperoxide antimalarials as platforms for targeted drug delivery.[5−9] Our designs in particular involve embedding a masked retro-Michael linker in an arterolane-like scaffold.[6−8] Intraparasitic reduction of the endoperoxide bond in such systems (e.g., **3**) serves to unmask a ketone and reveal the competent retro-Michael substrate **4**, which then undergoes traceless release of a 3″-carbamate-tethered payload (Scheme 1). The key reduction step is widely thought[10−13] to involve Fenton-type reaction in the parasite digestive vacuole (DV), promoted by iron(II)-heme that is

Received: July 22, 2015
Accepted: October 2, 2015
Published: October 2, 2015

DOI: 10.1021/acsmedchemlett.5b00296
ACS Med. Chem. Lett. 2015, 6, 1145−1149

Scheme 1. Trioxolane-Mediated Release of Mefloquine from Trioxolane Conjugate 3

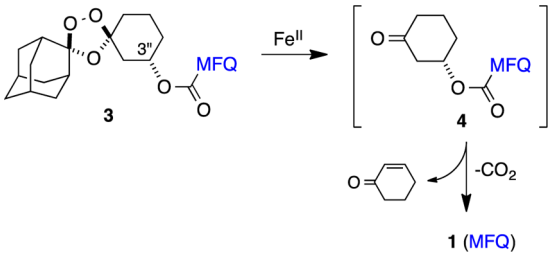

liberated during the catabolism of hemoglobin. However, our recent studies[8] demonstrating delivery of the antimetabolite puromycin to its ribosome target suggests that endoperoxide reduction in the parasite cytoplasm, promoted by labile ferrous iron[14] or perhaps by other cellular factors,[15] cannot be excluded as an alternate or additional site/mode of activation. These results also demonstrate that the scope of the approach extends beyond the delivery of other DV-acting agents.

For the particular application described herein, we envisioned that trioxolane-mediated delivery of **1** in the form **3** would reduce the exposure of free **1** in the brain since release of **1** should occur primarily within parasites, and the intact conjugate **3** was expected to exhibit poor brain penetration. If borne out, the approach might enable mefloquine to be more safely deployed, mitigating or eliminating its neuropsychiatric side effects. That the intrinsic potency of **1** is comparable to that of typical antimalarial trioxolanes (low nM) was another important consideration, given the necessarily stoichiometric nature of drug release. Finally, previous work had established that mefloquine exhibits synergistic antimalarial effects when combined with arterolane or an artemisinin.[15] Thus, several distinct factors augured for the potential utility of conjugate **3**.

The presence of a reactive amine in **1** made its incorporation in conjugate **3** straightforward. Thus, **3** was synthesized as a mixture of diastereomers in two steps from (±)-**5** and (±)-**1** (Scheme 2). Key intermediate **5**[16] was first converted to the *p*-nitrophenyl carbonate and then reacted with (±)-**1** to afford **3** in 63% overall yield. As we recently reported, *trans*-**5** is available from 3-hydroxycyclohexanone in a three-step process involving a diastereoselective Griesbaum co-ozonolysis reaction as the key step.[16] While this same process can yield single

Scheme 2. Synthesis of 3 and 6 from the Alcohol 5

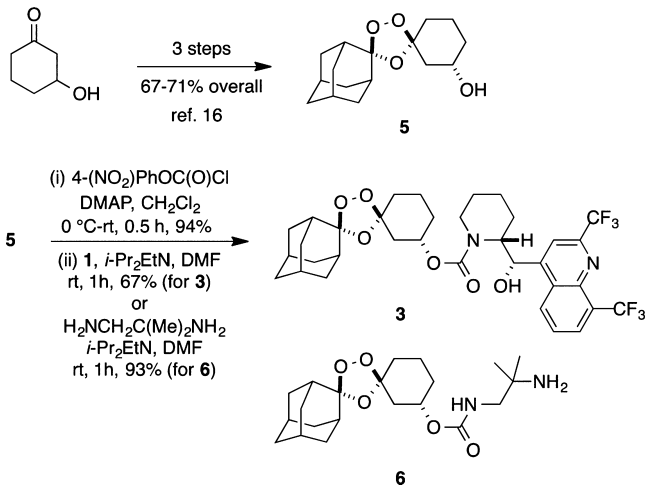

enantiomers of **5** when starting from nonracemic 3-hydroxycyclohexanone, (±)-**5** was employed for the studies reported herein. In a similar fashion, we prepared the conjugate **6**[16] to explore the effects of 3″-carbamate substitution in a trioxolane analogue more closely related to **2**.

The in vitro antiplasmodial activity of **1**, **2**, **3**, and **6** against chloroquine-resistant W2-strain *P. falciparum* parasites was assessed using a flow-cytometry-based growth inhibition assay.[17] All four compounds exhibited comparable, low-nM antiplasmodial activity that was superior to artemisinin (Table 1). While the combined application of **1** and **2** has been

Table 1. In Vitro Antimalarial Activity and Blood Stability of 1 and 3

		stability (%)[b]		
compd	W2 *P. falc.* EC_{50} ± SEM (nM)[a]	plasma	blood	B/P[d] ratio
1	2.5 ± 0.1	97	95	1.6
2	2.5 ± 0.7	n.d.	n.d.	1.5[18]
3	3.0 ± 0.6	94	85	0.7
6	2.7 ± 0.4	97[c]	n.d.	n.d.
ART[e]	9.3 ± 0.6	n.d.	n.d.	n.d.

[a]Mean of three (**1**, **3**, **ART**) or six (**2** and **6**) separate determinations. [b]Percent remaining after 240 min incubation in human plasma or whole blood. [c]Incubation for 120 min. [d]Apparent blood/plasma ratio. [e]Artemisinin control. n.d., not determined.

reported to be synergistic, it was not expected that **3** would necessarily exhibit greater potency than **1** or **2** alone since the mechanism by which **3** confers its two activities is not analogous to the combination of **1** and **2**. Even so, the excellent potency of 3″-carbamate analogues **3** and **6** does clearly demonstrate that trioxolane-based antiplasmodial effects can be realized with the hitherto underexplored 3″-substitution pattern.

The stability of **1** and its trioxolane conjugate **3** was also assessed in human plasma and whole blood. Neither compound showed detectable degradation in plasma when incubated at 37 °C for up to 4 h. Incubation of **3** in human whole blood did produce detectable amounts of released **1** that increased over time, indicating some blood-mediated conversion of **3** to **1**. Even so, ∼85% of **3** remained unchanged after 4 h in whole blood, suggesting more than sufficient stability for further in vivo evaluation. The blood/plasma ratio (B/P) of **3** was 0.7, less than that of either **1** or **2** (B/P ≈ 1.5), and more similar to the value of 0.8 reported for OZ439,[18] a 1,2,4-trioxolane that has shown pharmacokinetic properties superior to **2** in human clinical trials (Table 1).

With good antiplasmodial activity and blood stability established, we next compared the *in vivo* efficacy of **1**, **2**, **3**, and **6** in the *P. berghei* mouse model of malaria. Female Swiss-Webster mice (n = 5 per dosing arm) were inoculated with 10^6 *P. berghei* parasites and administered test compounds or vehicle by oral gavage once daily for 4 days. Parasitemia, morbidity, and mortality were evaluated daily over the 28 days of the study, with mice euthanized as required according to study protocols. The arterolane-like 3″-carbamate **6** and mefloquine (**1**) were the most effective treatments, with 4/5 mice in each cohort surviving to day 28 and exhibiting no detectable parasitemia (Figure 2). The excellent efficacy of **6** was highly encouraging and revealed the in vivo potential of trioxolane analogues with 3″-carbamate substitution. Indeed, compound **6** outperformed arterolane in this study (3/5 survivors in the cohort dosed with

DOI: 10.1021/acsmedchemlett.5b00296
ACS Med. Chem. Lett. 2015, 6, 1145−1149

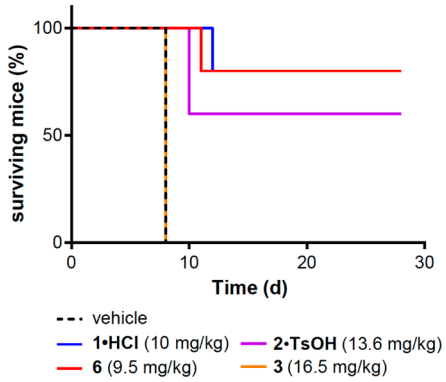

Figure 2. Survival time course of *P. berghei* infected mice treated by oral gavage at the indicated (equimolar) doses of test compound once daily for 4 days, starting on the day of inoculation.

arterolane tosylate). That **1** and **6** exhibited comparable in vivo efficacy at equimolar doses also confirmed **1** as an ideal payload for delivery from trioxolane conjugate **3**. Surprisingly, however, **3** proved to be entirely ineffective in this model (Figure 2). Comparing the results for 3″-carbamates **6** and **3**, we judged that the failure of **3** was most likely due to poor oral absorption, which was likely attributable to a molecular weight outside the ideal range. To explore this further and to test our original hypothesis that administration of **3** would exclude **1** from the brain, we evaluated the efficacy of **1** and **3** with intraperitoneal (i.p.) administration.

In an early in vivo study[19] of **1** using the *P. chabaudi* mouse malaria model, a single subcutaneous dose of 40 mg/kg was found to be curative. Using a similar model, we found that a single i.p. dose of just 10 mg/kg of **1** afforded parasitological cure at day 13 postinoculation (Table 2). Having thus established an effective i.p. dose of **1** in this model, we next evaluated its trioxolane conjugate **3** at equimolar (16.5 mg/kg) as well as at half-molar (8 mg/kg) and 3-fold higher (50 mg/kg) molar doses. We found that conjugate **3** was efficacious at both the 16.5 mg/kg (equimolar) and 50 mg/kg doses in this model, but not at the half-molar (8 mg/kg) dose (Table 2). These results confirmed our suspicions regarding the oral bioavailability of **3**, while also suggesting that **3** has reasonable pharmacokinetic properties once absorbed.

Table 2. Parasitemia of *P. chabaudi* Infected Mice Treated with a Single Intraperitoneal Dose of 1 or 3

		mean parasitemia ± SEM (%)		
cmpd	dose (mg/kg)	day 4[a]	day 7	day 13
vehicle		4.6 ± 0.5	34 ± 2.3	*b*
1	10	4.8 ± 0.5	0.02 ± 0.01	0
3	8	4.8 ± 0.4	33 ± 1.5	*b*
3	16.5	4.5 ± 1.1	0.7 ± 0.2	0.65 ± 0.65
3	50	5.4 ± 0.6	0	0

[a]Day postinoculation; animals dosed on day 4. [b]Animals sacrificed on day 8 due to poor health, as dictated by study protocol.

The promising in vitro and in vivo activities of **3** and **6** confirmed that 3″-substituted trioxolanes are able to access compartments of the parasite where endoperoxide activation occurs and trioxolane-based antiplasmodial effects are realized. To better understand the in vivo PK properties of **3** and its utility as a drug delivery platform for **1**, we performed a series of PK studies with **1** and **3** in infected and uninfected mice. In the first study, cohorts of *P. chaubaudi*-infected mice were treated with **1** (10 mg/kg i.p.) or with the trioxolane-conjugate **3** at the 3-fold higher molar dose (50 mg/kg i.p.). The higher dose of **3** was employed to increase the likelihood that detectable concentrations of released **1** could be measured in brain and plasma. We collected blood and brain samples over 24 h, and these were analyzed for concentrations of **1** and **3**. Comparing the plasma exposure-time course for **1** in these two cohorts reveals that administration of **1** in the form **3** significantly alters the plasma exposure profile of **1** (Figure 3). Thus, near-peak plasma concentrations of **1** were reached within 5 min in mice administered **1**, whereas plasma concentrations of **1** in mice receiving **3** were nearly undetectable at 30 min but then increased steadily out to 24 h (blue line, Figure 3).

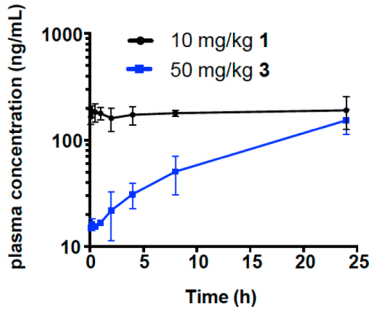

Figure 3. Plasma concentrations of **1** following a single i.p. dose of either **1** (10 mg/kg) or **3** (50 mg/kg) in *P. chabaudi* infected mice.

The full plasma and brain exposure profiles of **3** and **1** for **3**-treated mice are illustrated below (Figure 4). Thus, peak plasma concentrations of **3** are reached between 0.5 and 2 h, with some variability in t_{max} observed between individual mice. Peak plasma exposure is followed by slow clearance, with plasma levels of **3** falling to ~10% of peak values at 24 h. This sustained exposure profile is quite remarkable and atypical for a trioxolane, especially in an infected animal. By contrast to its high and sustained plasma exposure, **3** was entirely excluded from brain, as expected (orange dashed lines, Figure 4). Free **1** released from **3** was detected in both plasma and brain, and concentrations of **1** increased steadily over the 24 h study (blue lines, Figure 4). Significantly, brain concentrations of **1** were substantially lower at all time points in mice treated with 50 mg/kg of **3** than in mice administered a 3-fold lower molar

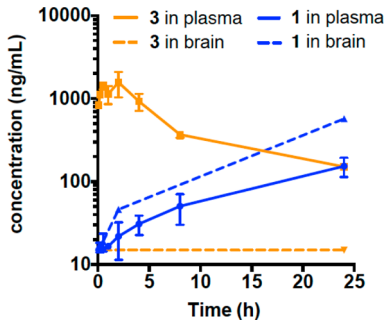

Figure 4. Time course of plasma and brain concentrations of **1** (blue) and **3** (orange) in *P. chabaudi* infected mice treated i.p. with 50 mg/kg **3**.

DOI: 10.1021/acsmedchemlett.5b00296
ACS Med. Chem. Lett. 2015, 6, 1145−1149

dose of **1** (Figure 5). Even allowing peak brain concentrations of **1** in **3**-treated mice to exceed by half again the levels at 24 h,

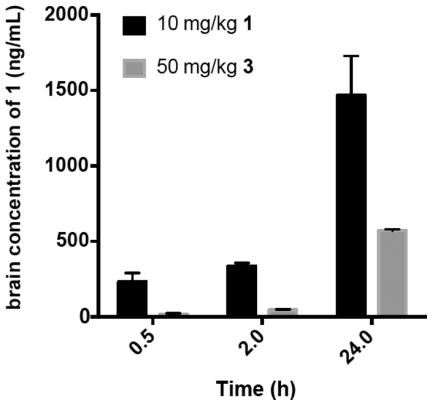

Figure 5. Brain concentrations of mefloquine (**1**) in *P. chabaudi* infected mice at three time points following i.p. administration of 10 mg/kg **1** (black bars) or 50 mg/kg **3** (gray bars).

we extrapolate a dose-corrected peak brain exposure of **1** in **3**-treated mice of ∼250 ng/mL, or just ∼18% that of **1**-treated mice at 24 h (∼1400 ng/mL). This represents a significant reduction in brain exposure that could plausibly mitigate off-target CNS effects.

The PK studies in infected mice revealed that conjugate **3** is excluded from brain as desired, but that some free **1** is released from **3** into systemic circulation where it eventually reaches the brain. What these initial PK studies could not address was the important question of how much **3** (and thus **1**) was actually delivered to *parasites* since only plasma and brain samples were analyzed in these PK studies. The collective pool of parasites in the infected mouse represents a notional "organ" that cannot be easily collected for analysis. Therefore, to estimate the extent to which **3** (and released **1**) partition into parasites in vivo, we performed an analogous study of **3** in *uninfected* animals, reasoning that the difference in plasma drug exposure between infected and uninfected cohorts would reflect the amount of **3** delivered to parasites (and thus unobservable) in the infected animals. Interestingly, the overall plasma AUC of **3** was found to be ∼2.5-fold higher in uninfected vs infected animals (Table 3), the difference providing a rough estimate of the total exposure of **3** within parasites of the infected animals (AUC ≈ 20,500 h·ng/mL). An alternate interpretation that **3** is more rapidly degraded by free, systemic ferrous iron present only in infected animals is inconsistent with our finding that plasma concentrations of released **1** were comparable in both infected and uninfected animals receiving **3** (Supplemental Figure S1). Additionally, our observation that the volume of distribution of **3** is ∼2.5-fold higher in the infected animal is consistent with the accumulation of **3** in an additional compartment that is present only in infected animals (i.e., parasitized erythrocytes). Thus, our PK data suggest that conjugate **3** is excluded from brain in mice and distributed primarily (∼60−70%) in parasitized erythrocytes. The remainder of **3** remains systemically available, and some fraction of this material is converted to **1** by a mechanism that is, as yet, undetermined but that occurs to a similar extent in infected and uninfected animals.

Table 3. Noncompartmental Pharmacokinetic Parameters for 3 in Plasma Following i.p. Administration of 50 mg/kg in Uninfected or Infected Mice

parameter	units	uninfected	infected
terminal $t_{1/2}$	h	8.41	8.60
t_{max}	h	1.00	2.00
C_{max}	ng/mL	3620	1570
AUC_{inf}	h·ng/mL	34100	13600
CL/F	mL/h/kg	1470	3670
dose/C_{max}	L/kg	13.8	31.8
V_z/F	L/kg	17.8	45.5
MRT_{last}	h	6.93	6.43
MRT_{inf}	h	11.0	10.6

It has been suggested[1] that the development of nonracemic forms of **1** could mitigate the CNS side effects of (±)-**1**. It is not altogether clear this should be the case, however, in light of more recent studies[3] showing that (+)-**1** or (−)-**1** (or both) interact with an array of potential CNS off-targets. Thus, therapeutic approaches that mitigate the overall exposure of **1** in brain would appear to hold greater promise for mitigating the neuropsychiatric effects of **1**. It is thus significant that trioxolane-mediated delivery of **1** in the form **3**, as detailed herein, significantly reduces brain exposure in mice at efficacious doses. Also noteworthy is that the presence of **1** in **3** appears to confer favorable in vivo properties that can be attributed to intrinsic PK properties of **1** (i.e., long half-life and mean residence time, and high volume of distribution). Thus, the same PK properties that have made **1** an effective chemoprophylactic are also exhibited by its trioxolane conjugate **3**. At the same time, the physiochemical properties that likely serve to exclude **3** from the brain (high MW and polar surface area) appear also to limit oral bioavailability. An effective oral formulation of **3** might still be identified if poor solubility and not poor intrinsic permeability is the problem. Alternatively, slow release of the conjugate from an injectable polymer matrix may represent an ideal means to deploy **3** for chemoprophylaxis and/or in the context of malaria elimination and eradication campaigns where the emphasis is on patient adherence and drug tolerability. More generally, our results with **3** provide additional evidence[7] in support of trioxolane-mediated drug delivery as a purely chemical means to achieve cell/tissue-selective drug targeting.

■ ASSOCIATED CONTENT

Supporting Information

The Supporting Information is available free of charge on the ACS Publications website at DOI: 10.1021/acsmedchemlett.5b00296.

Experimental procedures, supplemental data and figures, and copies of NMR spectra for new compounds (PDF)

■ AUTHOR INFORMATION

Corresponding Author

*E-mail: adam.renslo@ucsf.edu.

Present Addresses

⊥BASF SE, Carl-Bosch Strasse 38, 67056 Ludwigshafen am Rhein, Germany.

#ProLynx, LLC, San Francisco California 94158, United States.

Author Contributions

The manuscript was written through contributions of all authors. All authors have given approval to the final version of the manuscript.

DOI: 10.1021/acsmedchemlett.5b00296
ACS Med. Chem. Lett. 2015, 6, 1145−1149

Funding

A.R.R. acknowledges the support of the US National Institutes of Health (AI105106). The work preformed by H.L. and M.B. was supported by a subcontract on AI105106.

Notes

The authors declare no competing financial interest.

■ ACKNOWLEDGMENTS

Bioanalysis of plasma and brain samples was performed at Integrated Analytical Solutions (Berkeley, CA). We thank Alan Wolfe (UCSF) for helpful discussions and for calculating the pharmacokinetic parameters in Table 3.

■ ABBREVIATIONS

CNS, central nervous system; DMAP, 4-dimethylaminopyridine; SEM, standard error in mean; PK, pharmacokinetic; AUC, area under the curve; Cl, clearance; F, fraction of drug achieving systemic exposure following the i.p. dose; Vz, volume of distribution; MRT, mean residence time

■ REFERENCES

(1) Schmidt, M.; Sun, H.; Rogne, P.; Scriba, G. K. E.; Griesinger, C.; Kuhn, L. T.; Reinscheid, U. M. Determining the Absolute Configuration of (+)-Mefloquine HCl, the Side-Effect-Reducing Enantiomer of the Antimalaria Drug Lariam. *J. Am. Chem. Soc.* **2012**, *134*, 3080−3083.

(2) Karle, J. M.; Karle, I. L. Crystal Structure of (−)-Mefloquine Hydrochloride Reveals Consistency of Configuration with Biological Activity. *Antimicrob. Agents Chemother.* **2002**, *46*, 1529−1534.

(3) Janowsky, A.; Eshleman, A. J.; Johnson, R. A.; Wolfrum, K. M.; Hinrichs, D. J.; Yang, J.; Zabriskie, T. M.; Smilkstein, M. J.; Riscoe, M. K. Mefloquine and Psychotomimetics Share Neurotransmitter Receptor and Transporter Interactions in Vitro. *Psychopharmacology* **2014**, *231*, 2771−2783.

(4) Vennerstrom, J. L.; Arbe-Barnes, S.; Brun, R.; Charman, S. A.; Chiu, F. C. K.; Chollet, J.; Dong, Y.; Dorn, A.; Hunziker, D.; Matile, H.; McIntosh, K.; Padmanilayam, M.; Santo Tomas, J.; Scheurer, C.; Scorneaux, B.; Tang, Y.; Urwyler, H.; Wittlin, S.; Charman, W. N. Identification of an Antimalarial Synthetic Trioxolane Drug Development Candidate. *Nature* **2004**, *430*, 900−904.

(5) Gibbons, P.; Verissimo, E.; Araujo, N. C.; Barton, V.; Nixon, G. L.; Amewu, R. K.; Chadwick, J.; Stocks, P. A.; Biagini, G. A.; Srivastava, A.; Rosenthal, P. J.; Gut, J.; Guedes, R. C.; Moreira, R.; Sharma, R.; Berry, N.; Cristiano, M. L. S.; Shone, A. E.; Ward, S. A.; O'Neill, P. M. Endoperoxide Carbonyl Falcipain 2/3 Inhibitor Hybrids: Toward Combination Chemotherapy of Malaria Through a Single Chemical Entity. *J. Med. Chem.* **2010**, *53*, 8202−8206.

(6) Mahajan, S. S.; Deu, E.; Lauterwasser, E. M. W.; Leyva, M. J.; Ellman, J. A.; Bogyo, M.; Renslo, A. R. A Fragmenting Hybrid Approach for Targeted Delivery of Multiple Therapeutic Agents to the Malaria Parasite. *ChemMedChem* **2011**, *6*, 415−419.

(7) Deu, E.; Chen, I.; Lauterwasser, E. M. W.; Valderramos, J.; Li, H.; Edgington, L.; Renslo, A. R.; Bogyo, M. Ferrous Iron-dependent Drug Delivery Enables Controlled and Selective Release of Therapeutic Agents in Vivo. *Proc. Natl. Acad. Sci. U. S. A.* **2013**, *110*, 18244−18249.

(8) Fontaine, S. D.; Spangler, B.; Gut, J.; Lauterwasser, E. M. W.; Rosenthal, P. J.; Renslo, A. R. Drug Delivery to the Malaria Parasite Using an Arterolane-like Scaffold. *ChemMedChem* **2015**, *10*, 47−51.

(9) Oliveira, R.; Newton, A. S.; Guedes, R. C.; Miranda, D.; Amewu, R. K.; Srivastava, A.; Gut, J.; Rosenthal, P. J.; O'Neill, P. M.; Ward, S. a; Lopes, F.; Moreira, R. An Endoperoxide-based Hybrid Approach to Deliver Falcipain Inhibitors Inside Malaria Parasites. *ChemMedChem* **2013**, *8*, 1528−1536.

(10) Creek, D. J.; Charman, W. N.; Chiu, F. C. K.; Prankerd, R. J.; Dong, Y.; Vennerstrom, J. L.; Charman, S. A. Relationship Between Antimalarial Activity and Heme Alkylation for Spiro- and Dispiro-1,2,4-trioxolane Antimalarials. *Antimicrob. Agents Chemother.* **2008**, *52*, 1291−1296.

(11) O'Neill, P. M.; Posner, G. H. A Medicinal Chemistry Perspective on Artemisinin and Related Endoperoxides. *J. Med. Chem.* **2004**, *47*, 2945−2964.

(12) Hartwig, C. L.; Lauterwasser, E. M. W.; Mahajan, S. S.; Hoke, J. M.; Cooper, R. A.; Renslo, A. R. Investigating the Antimalarial Action of 1,2,4-Trioxolanes with Fluorescent Chemical Probes. *J. Med. Chem.* **2011**, *54*, 8207−8213.

(13) Robert, A.; Benoit-Vical, F.; Claparols, C.; Meunier, B. The Antimalarial Drug Artemisinin Alkylates Heme in Infected Mice. *Proc. Natl. Acad. Sci. U. S. A.* **2005**, *102*, 13676−13680.

(14) Stocks, P. A.; Bray, P. G.; Barton, V. E.; Al-Helal, M.; Jones, M.; Araujo, N. C.; Gibbons, P.; Ward, S. A.; Hughes, R. H.; Biagini, G. A.; Davies, J.; Amewu, R.; Mercer, A. E.; Ellis, G.; O'Neill, P. M. Evidence for a Common Non-heme Chelatable-iron-dependent Activation Mechanism for Semisynthetic and Synthetic Endoperoxide Antimalarial Drugs. *Angew. Chem., Int. Ed.* **2007**, *46*, 6278−6283.

(15) Haynes, R. K.; Cheu, K.-W.; Chan, H.-W.; Wong, H.-N.; Li, K.-Y.; Tang, M. M.-K.; Chen, M.-J.; Guo, Z.-F.; Guo, Z.-H.; Sinniah, K.; Witte, A. B.; Coghi, P.; Monti, D. Interactions Between Artemisinins and Other Antimalarial Drugs in Relation to the Cofactor Model − a Unifying Proposal for Drug Action. *ChemMedChem* **2012**, *7*, 2204−2226.

(16) Fontaine, S. D.; Dipasquale, A. G.; Renslo, A. R. Efficient and Stereocontrolled Synthesis of 1,2,4-Trioxolanes Useful for Ferrous Iron-Dependent Drug Delivery. *Org. Lett.* **2014**, *16*, 5776−5779.

(17) Sijwali, P. S.; Kato, K.; Seydel, K. B.; Gut, J.; Lehman, J.; Klemba, M.; Goldberg, D. E.; Miller, L. H.; Rosenthal, P. J. Plasmodium Falciparum Cysteine Protease Falcipain-1 Is Not Essential in Erythrocytic Stage Malaria Parasites. *Proc. Natl. Acad. Sci. U. S. A.* **2004**, *101*, 8721−8726.

(18) Charman, S. A.; Arbe-Barnes, S.; Bathurst, I. C.; Brun, R.; Campbell, M.; Charman, W. N.; Chiu, F. C. K.; Chollet, J.; Craft, J. C.; Creek, D. J.; Dong, Y.; Matile, H.; Maurer, M.; Morizzi, J.; Nguyen, T.; Papastogiannidis, P.; Scheurer, C.; Shackleford, D. M.; Sriraghavan, K.; Stingelin, L.; Tang, Y.; Urwyler, H.; Wang, X.; White, K. L.; Wittlin, S.; Zhou, L.; Vennerstrom, J. L. Synthetic Ozonide Drug Candidate OZ439 Offers New Hope for a Single-dose Cure of Uncomplicated Malaria. *Proc. Natl. Acad. Sci. U. S. A.* **2011**, *108*, 4400−4405.

(19) Sweeney, T. R. Efficacy of Mefloquine Against Malaria Parasites in Animal Models. *W.H.O. Technol. Rep. Ser.* **1982**, *82*, 981.

DOI: 10.1021/acsmedchemlett.5b00296
ACS Med. Chem. Lett. 2015, 6, 1145−1149